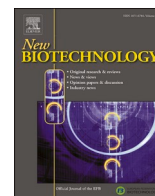


Contents lists available at [ScienceDirect](https://www.sciencedirect.com)

New BIOTECHNOLOGY

journal homepage: www.elsevier.com/locate/nbt

A wide array of lignin-related phenolics are oxidized by an evolved bacterial dye-decolourising peroxidase

Diogo Silva^a, Ana Catarina Sousa^{b,c}, M. Paula Robalo^{b,c,*}, Lúgia O. Martins^{a,**}

^a Institute of Chemical and Biological Technology António Xavier, NOVA New University of Lisbon, Av da República, 2780-157 Oeiras, Portugal

^b Department of Chemical Engineering, Instituto Superior de Engenharia de Lisboa, Polytechnic Institute of Lisbon, R. Conselheiro Emídio Navarro, 1, 1959-007 Lisboa, Portugal

^c Centre for Structural Chemistry, Institute of Molecular Sciences, Complexo I; Instituto Superior Técnico, University of Lisbon, Av. Rovisco Pais, 1049-001 Lisboa, Portugal

ARTICLE INFO

Keywords:

Oxidoreductases
Biocatalysis
Biorefineries
Lignin valorization
Lignans
Natural products

ABSTRACT

Lignin is the second most abundant natural polymer next to cellulose and by far the largest renewable source of aromatic compounds on the planet. Dye-decolourising peroxidases (DyPs) are biocatalysts with immense potential in lignocellulose biorefineries to valorize emerging lignin building blocks for environmentally friendly chemicals and materials. This work investigates the catalytic potential of the engineered PpDyP variant 6E10 for the oxidation of 24 syringyl, guaiacyl and hydroxybenzene lignin-phenolic derivatives. Variant 6E10 exhibited up to 100-fold higher oxidation rates at pH 8 for all the tested phenolic substrates compared to the wild-type enzyme and other acidic DyPs described in the literature. The main products of reactions were dimeric isomers with molecular weights of $(2 \times MW_{\text{substrate}} - 2H)$. Their structure depends on the substitution pattern of the aromatic ring of substrates, i.e., of the coupling possibilities of the primarily formed radicals upon enzymatic oxidation. Among the dimers identified were syringaresinol, divanillin and diapocynin, important sources of structural scaffolds exploitable in medicinal chemistry, food additives and polymers.

1. Introduction

Dye-decolourising peroxidases (DyPs) are microbial peroxidases capable of efficient oxidation of a set of structurally diverse substrates, including synthetic dyes, aromatic sulfides, metals, phenolic and non-phenolic lignin units, showing attractive catalytic properties for biotechnological applications [1,2]. Their ability to oxidize lignin-related compounds, together with their abundance in genomes of lignin-degrading basidiomycetes (white-rot fungi) [3–5] and widespread presence in fungal transcriptomes inhabiting forest soils [6], support an active contribution to lignin biodegradation and conversion enzymatic systems.

The pulp and paper industry produces about 50 M tons of lignin annually, but most of it is burned for energy; only 1 M tons reach the chemicals market [7,8]. Lignin is currently used for low- and

medium-value applications (e.g. binding and dispersing agents), with energy accounting for around 89% of the market. The recent implementation of novel strategies for lignin depolymerization, involving electrochemistry, photocatalysis, heterogeneous catalysis and ionic liquids, has allowed well-defined fractions to be obtained in acceptable quantities [7,9–12], starting new value chains from the lignin-derived phenolic platform of chemicals (Scheme 1). Lignin-derived chemicals can significantly impact every aspect of life [13–17]. The dimerization of phenolic compounds via oxidative coupling using oxidoreductases, such as laccases and peroxidases, can generate the central motif of lignans and neolignans, multifunctional compounds [18–23] extracted from plants at low yields, which have been traditionally used as antioxidants, antitumor, antiinflammatory, antineurodegenerative, antiviral, and antimicrobial agents [24]. Furthermore, the functionalization of the hydroxyl groups of lignin-related phenolics can result in polymer

Abbreviations: DyP, Dye decolourising peroxidase; DMP, 2,6-dimethoxyphenol; NHE, normal hydrogen electrode; CV, cyclic voltammetry; E_{pa} , anodic peak potential; E_{pc} , cathodic peak potential ().

* Corresponding author at: Department of Chemical Engineering, Instituto Superior de Engenharia de Lisboa, Polytechnic Institute of Lisbon, R. Conselheiro Emídio Navarro, 1, 1959-007 Lisboa, Portugal.

** Corresponding author.

E-mail addresses: mprobalo@deq.isel.ipl.pt (M.P. Robalo), lmartins@itqb.unl.pt (L.O. Martins).

<https://doi.org/10.1016/j.nbt.2022.12.003>

Received 12 November 2022; Received in revised form 12 December 2022; Accepted 19 December 2022

Available online 20 December 2022

1871-6784/© 2022 The Author(s). Published by Elsevier B.V. This is an open access article under the CC BY-NC-ND license (<http://creativecommons.org/licenses/by-nc-nd/4.0/>).

building blocks, with vanillin, ferulic acid, guaiacol, syringaldehyde or 4-hydroxybenzoic acid topping the list of the most used lignin derivatives for these purposes [7]. Notably, aromatic lignin units offer rigidity, hydrophobicity and fire resistance in a polymeric backbone, such as thermosets, including vinyl ester, cyanate ester, epoxy and benzoxazine resins, as well as thermoplastics, including polyesters, poly-anhydrides, Schiff base polymers, polyacetals, polyoxalates, polycarbonates and acrylate polymers [25–28]. Therefore, the current challenge is the set of economic, sustainable and waste-free bioprocesses that allow the full implementation of lignin as starting material for the production of drop-in chemicals, polymers and other emerging functional materials [7,13–16].

Pseudomonas putida MET94 PpDyP is an enzyme that oxidizes anthraquinone and azo dyes with high efficiency, as well as metal ions and phenolic and non-phenolic lignin-related compounds [29]. A directed evolution approach resulted in a PpDyP-engineered variant, 6E10, displaying improved catalytic efficiency towards the lignin-related phenol 2,6-dimethoxyphenol (DMP, a.k.a. syringol), a shift in pH optima from 4.3 to 8, and an increased resistance to H₂O₂ inhibition [30]. The substrate range of 6E10 was previously investigated using a few phenolics, including guaiacylglycerol- β -guaiacyl ether, Kraft lignin and aromatic amine substrates [30]. The products obtained from the oxidation of the aromatic amines were identified using ESI-MS, showing the generation of substituted benzoquinonediimine trimeric structures and phenazine cores, important biological motifs of antibiotics, and antibacterial agents, among other biotechnologically interesting compounds. In this work, the substrate scope of 6E10 for lignin-related substrates was further investigated by screening 24 lignin-derived phenolic compounds from the *p*-hydroxyphenyl, syringyl and guaiacyl types. The products of selected reactions were identified, revealing the enzyme's potential for biotechnological applications.

2. Material and methods

2.1. Enzymes and chemicals

Recombinant wild-type PpDyP and evolved variant 6E10 were produced and purified as previously described [29,30]. Acetosyringone, syringaldehyde, acetovanillone, vanillyl alcohol, guaiacol, vanillin,

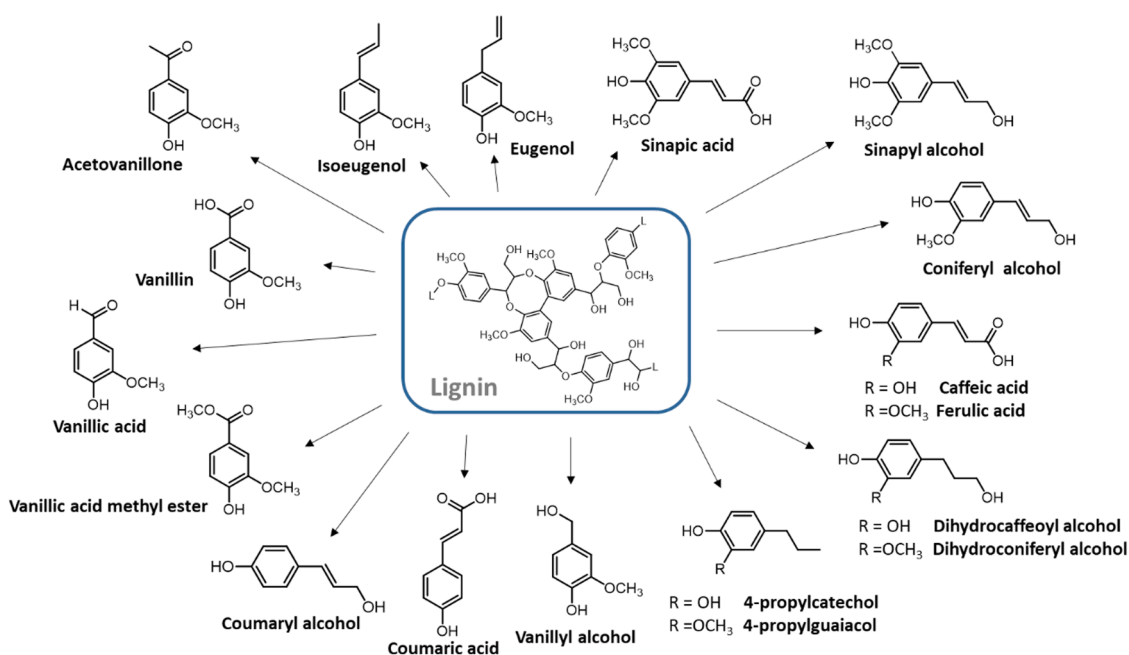
ferulic acid, coniferyl aldehyde, 4-hydroxy acetophenone, caffeic acid, and *p/m/o*- coumaric acids were from Sigma-Aldrich (Burlington, MA, USA). Syringol, methyl syringate, sinapic acid, and syringic acid were from Alfa Aesar (Ward Hill, MA, USA). Gallic acid was from Merck (Darmstadt, Germany), and vanillic acid was from Fluka Chemicals (Buchs, Switzerland).

2.2. Cyclic voltammetry measurements

The redox potentials of the phenolics tested were measured using an EG&G Princeton Applied Research (PAR) Model 273 A potentiostat/galvanostat (Princeton, USA) monitored with Electrochemistry PowerSuite v2.51 software from PAR. Cyclic voltammograms of 1 mM of phenolics in 0.1 M acetate (pH 4) and phosphate (pH 8) buffers were obtained using a three-electrode configuration cell with a glassy carbon (GC) disk working electrode (3.0 mm diameter, Radiometer analytical, SAS, Lyon, France), a platinum wire counter electrode and an aqueous Ag/AgCl/saturated KCl reference electrode (Radiometer analytical). For aqueous insoluble compounds, 10% ethanol (v/v) was added. The working electrode was carefully polished with alumina powder before each measurement. The potential was scanned from -0.3 – 1.4 V at a scan rate of 100 mV/s. All measurements were performed at room temperature (RT), and the solutions were flushed with dinitrogen before use. The measured potentials were corrected by $+0.197$ V to the normal hydrogen electrode (NHE).

2.3. UV-visible spectra and determination of molar extinction coefficients of phenolic compounds

The UV-visible absorption spectra of phenolic compounds were recorded in 0.1 M citrate buffer, pH 4, and 0.1 M phosphate buffer, pH 8, in the wavelength range 200–900 nm, using a Synergy 2 (Biotek Instruments, Vermont, USA) microtiter plate reader. The molar extinction coefficients (in the concentration range of 10–200 μ M) were determined at their maximal wavelengths using the Lambert-Beer law ($A = \epsilon \times l \times c$; where A is the absorbance, l the optical length (0.65 cm) and c the compound concentration) (Supplementary Table S1) at pH 4 and pH 8 using a Synergy 2, (Biotek Instruments), 96-well microplate reader.



Scheme 1. Phenolic lignin units available from biorefineries [7].

2.4. Assays of enzymatic activity of PpDyP and 6E10

Enzymatic reactions were performed in 96 well plates at 30 °C with 0.5 mM of each substrate at 0.1 M citrate buffer, pH 4, for reactions with wild-type PpDyP (0.2 mg/mL in the reaction), and 0.1 M phosphate buffer, pH 8, for reactions with variant 6E10 (0.1 mg/mL in the reaction). Reactions were started by adding 0.5 mM H₂O₂ and were monitored at each substrate's maximal wavelength, except for syringol and guaiacol, where product formation was monitored (Supplementary Table S1). Apparent steady-state kinetic parameters were measured at substrate concentrations from 0.01 to 0.5 mM in the presence of 0.5 mM H₂O₂.

2.5. High-performance liquid chromatography (HPLC)

Reactions were set up using 0.1 M citrate buffer, pH 4, for wild-type and 0.1 M phosphate buffer, pH 8.0, for 6E10, with 0.5 mM of each substrate. The addition of 0.5 mM H₂O₂ started reactions and after 24 h they were stopped with 50% methanol before injection. Enzymatic oxidation was monitored by HPLC performed using a Waters Alliance (Milford, MA, USA) 2695 HPLC System with a Purospher STAR RP-18e column (125 × 4 mm), 5 μm particle size (Merck KGaA, Darmstadt, Germany), at 40 °C and a flow rate of 1.0 mL·min⁻¹. Reaction products were eluted with a linear gradient of H₂O/methanol plus 0.5% acetic acid (solvent A) from 30% to 80% of methanol over 25 min. They were maintained isocratic for 10 min, then returned to initial conditions for 2 min and maintained isocratic for 8 min. Absorption was monitored between 200 and 500 nm by a Waters Photodiode Array Detector 2996 operated by Empower Pro, version 5, 2002 (Waters Chromatography, Milford, MA, USA).

2.6. Enzymatic reactions for identification of products by mass spectrometry (MS)

The enzymatic reactions (0.5 mM substrate) were performed at RT in a total volume of 1 mL, using 100 mM NH₄HCO₃ buffer at pH 8, 6E10 (1 U/mL) and 0.5 mM H₂O₂, for 1 h. The reactions were stopped by addition of methanol in a similar volume to the volume of the reaction, centrifuged, and the soluble fraction stored at 4 °C until MS analysis. A 20 mg/mL sample solution was prepared in water (Optima™ LC/MS Grade, Fisher Scientific, Waltham, MA, USA) and further diluted to 1:100 in 50% methanol (Optima™ LC/MS Grade, Fisher Scientific), 1 μL was injected on the column. Chromatographic analysis was performed on an UltiMate 3000 UHPLC (Thermo Fisher Scientific, Waltham, MA, USA). The separation was performed using a Waters XBridge column C18 (2.1 × 150 mm, 3.5 μm particle size, P/N 186003023). The mobile phase A was water with 0.1% formic acid (v/v), and mobile phase B was acetonitrile with 0.1% formic acid (v/v) (Optima™ LC/MS Grade, Fisher Scientific). The column temperature was maintained at 30 °C, and a flow rate of 400 μL/min was used. The data was acquired on a Q Exactive Focus (Thermo Fisher Scientific) coupled to UHPLC, using Xcalibur software v.4.0.27.19 (Thermo Fisher Scientific). The method consisted of several cycles of Full MS scans (R= 70,000) in positive mode. External calibration was performed using Linear Ion Trap (LTQ) electrospray ionization (ESI) Positive Ion Calibration Solution (Thermo Fisher Scientific). The raw MS data were analyzed using Qual Browser Xcalibur software v4.0 (Thermo Fisher Scientific). Data was provided by the Mass Spectrometry Unit (UniMS), ITQB/iBET, Oeiras, Portugal.

2.7. Enzymatic reactions for identification of products by ¹H NMR

The enzymatic reactions (5 mM substrate) were performed at RT in a total volume of 10 mL, using 100 mM potassium phosphate buffer at pH 8, 6E10 (5 U/mL) and 5 mM H₂O₂ for 1 h. The reactions were stopped by addition of methanol, and the solvent was evaporated using a Büchi Rotavapor R-205 (Flawil, Switzerland). The residues were resuspended

in methanol, filtered, and the solvent evaporated for ¹H NMR analysis. ¹H NMR spectra were recorded on a Bruker Avance (400 MHz) spectrometer (Billerica, MA, USA) in CD₃OD-d₄ as a solvent with a 5 mm probe. Signals were referenced to the residual signal of the deuterated solvent.

3. Results and discussion

3.1. Electrochemical characterization of lignin-related phenolic substrates

The 24 phenolic compounds selected are good representatives of the three classes of lignin-related phenolics: syringyl-type phenolics, with methoxy substituents in both *ortho* positions, guaiacyl-type phenolics, with a single methoxy group, and hydroxyl benzenes (Table 1). The electrochemical data in the literature for these compounds are hardly comparable insofar as they were measured at variable scan rates and pH values, and in the presence of different organic solvents and electrolyte concentrations. Therefore, the redox potential for all compounds tested was determined, considering their structural diversity and the redox potential dependence on phenolic structural characteristics.

The one-electron oxidation of phenols is a dissociative electron transfer and involves the loss of a proton: PhOH + H₂O → PhO⁻ + H₃O⁺ + e⁻, and therefore, their redox potentials are pH-dependent. The oxidation of phenolate ions results in the formation of phenoxyl radicals: PhO⁻ → PhO[•] + e⁻. The electrochemical studies were performed for all phenolic compounds at pH 4 and 8, the optimal values for wild-type PpDyP and variant 6E10, respectively (Table 2). The cyclic voltammograms of the phenolic compounds displayed one well-defined anodic peak and after the oxidation no reverse peak was observed (Supplementary Fig S1). The absence of a cathodic peak in the reverse scan indicates that the oxidized generated species are involved in chemical reactions and rapidly removed from the medium. The exceptions are with syringaldehyde, acetosyringone, and methyl syringate, where a cathodic wave was observed, although in an irreversible process (Table 2 and Supplementary Fig S2).

The oxidation potentials of phenolics at pH 8 are lower than at pH 4, which relates to the proximity to the pK_a values of most phenolics (Table 2); due to the higher concentrations of the phenolate ions at pH 8, they are more prone to be oxidized than the corresponding phenolic group [31]. The oxidation potentials follow the trend of syringyl < guaiacyl < hydroxybenzene (Table 2), and the presence and positions of substituents on the aromatic ring directly affect redox potentials. The oxidation is easier when electron-donating groups (e.g. Me, OMe, OH) are present; these groups might induce radical stabilization resulting in a decrease in redox potential, while the presence of electron-withdrawing functionalities (e.g. COR, R=H, CH₃, OH, OCH₃) has the opposite effect. The electron-withdrawing effect of COR groups at the *para* position is evident in both syringyl and guaiacyl-type groups (Tables 1 and 2); they release electron density from the aromatic ring, deactivating the phenol group that becomes less available for electron release and more difficult to oxidize. Different substituents show different acceptor capabilities depending on the phenolic family. However, no significant differences were found; the syringyl type show anodic peak potential (E_{pa}) values between 0.87 and 1.06 V, and the guaiacyl type from 1.09 to 1.17 V (Table 2). The relative position of the other substituents to the phenol group can also be decisive, as illustrated by the coumaric acid series: *o*- and *m*-coumaric acids showed higher anodic potentials than the corresponding *para* isomer, which is the easiest to oxidize, probably due to hyperconjugation between the aromatic ring and the CH=CHCOOH group. The introduction of methoxy groups in the *ortho* positions lowers the E_{pa} values (Table 2), as is evidenced by the comparison of values for acetosyringone (1.04 V), acetovanillone (1.12 V), and 4-hydroxyacetophenone (1.3 V). This is probably due to the conjugative electron donation of the OCH₃ group and the stabilization of the intermediate. The effect of a conjugated double bond is evidenced by the lowest oxidation potentials measured for coniferyl alcohol, coniferyl aldehyde

Table 1
Structure of the lignin-phenolic compounds investigated in this work.

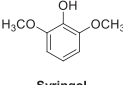
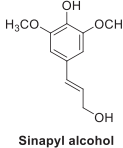
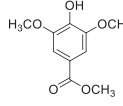
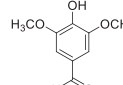
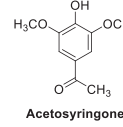
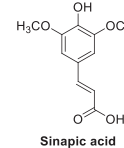
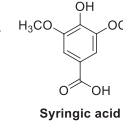
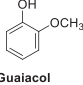
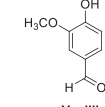
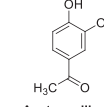
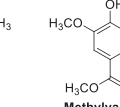
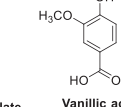
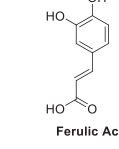
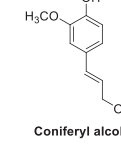
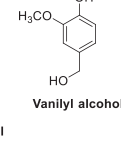
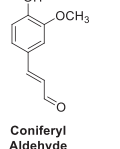
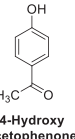
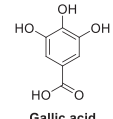
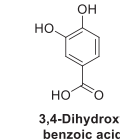
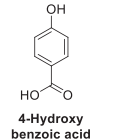
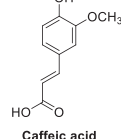
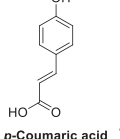
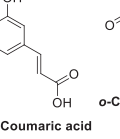
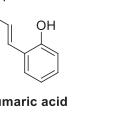
Syringil-type phenolics									
									
Syringol	Sinapyl alcohol	Methylsyringate	Syringaldehyde	Acetosyringone	Sinapic acid	Syringic acid			
Guaiacyl-type phenolics									
									
Guaiacol	Vanillin	Acetovanillone	Methylvanillate	Vanillic acid	Ferulic Acid	Coniferyl alcohol	Vanillyl alcohol	Coniferyl Aldehyde	
Hydroxybenzene-type phenolics									
									
4-Hydroxy acetophenone	Gallic acid	3,4-Dihydroxy benzoic acid	4-Hydroxy benzoic acid	Caffeic acid	p-Coumaric acid	m-Coumaric acid	o-Coumaric acid		

Table 2
Electrochemical data of lignin-related phenolics vs. NHE in buffered solutions (100 mM acetate, pH 4 and 100 mM phosphate, pH 8) at a scan rate of 100 mV/s.

Lignin-related phenolics	pKa	pH 4		pH 8	
		E _{pa} (V)	E _{pc} (V)	E _{pa} (V)	E _{pc} (V)
Syringyl-type phenolics					
Syringol	9.9 ^a	0.76	–	0.69	–
Sinapyl alcohol	9.4 ^b	0.77	–	–	–
Acetosyringone	7.9 ^a	1.04	–	0.71 ³	0.56 ³
		–		1.31	–
Methyl syringate	8.7 ^a	0.99	–	0.68 ¹	0.60 ¹
Syringaldehyde	7.3 ^a	1.06	0.78	0.76 ²	0.60 ²
Sinapic acid	9.2 ^a	0.82	–	0.63	–
Syringic acid	7.8 ^c	0.87	–	–	–
Guaiacyl-type phenolics					
Coniferyl alcohol	9.5 ^a	0.82	–	0.69	–
Vanillin	7.4 ^a	1.14	–	0.86	–
Coniferyl aldehyde	7.9 ^a	0.96	–	0.68	–
Ferulic acid	9.4 ^a	0.94	–	0.73	–
Methyl vanillate	8.4 ^d	1.17	–	0.86	–
Vanillyl alcohol	9.8 ^a	1.01	–	0.9	–
Acetovanillone	7.8 ^a	1.12	–	0.89	–
Guaiacol	9.9 ^a	1.06	–	0.83	–
Vanillic acid	8.5 ^c	1.09	–	–	–
Hydroxybenzene-type phenolics					
Caffeic acid	8.6 ^e	–	–	0.72	–
m-Coumaric acid	10.4 ^f	1.22	–	1.05	–
p-Coumaric acid	9.9 ^f	1.06	–	0.89	–
o-Coumaric acid	9.6 ^f	1.12	–	0.94	–
3,4-hydroxybenzoic acid	–	1.00	–	0.94	–
4-hydroxybenzoic acid	8.7 ^c	–	–	–	–
Gallic acid	12.2 ^c	–	–	–	–
4-hydroxyacetophenone	8.1 ^d	1.3	–	1.17	–

¹) E_{1/2} = 0.64 V; ΔE = 80 mV; I_c/I_a = 0.7;

²) E_{1/2} = 0.68 V; ΔE = 160 mV; I_c/I_a = 0.7;

³) E_{1/2} = 0.64 V; ΔE = 150 mV; I_c/I_a = 1.0.

^a [32]; ^b <https://foodb.ca/compounds/>; ^c [33]; ^d <https://www.chemicalbook.com/>; ^e [34]; ^f [35].

and sinapic acid when compared with vanillyl alcohol, vanillin and syringic acid, respectively (Table 2). The syringyl-type counterparts, sinapyl alcohol and sinapic acid are the most easily oxidized

compounds.

3.2. Conversion yields of lignin-related phenolics

HPLC estimated the substrate conversions after 24 h of reaction at RT. Both enzymes converted all substrates, but 6E10 showed improved yields (from 10% to 75%) across the syringyl, guaiacyl and hydroxybenzene-type families (Fig. 1 and Supplementary Table S2). Wild-type converted ≥ 98% of sinapic acid and coniferyl alcohol, for example. In contrast, the 6E10 variant converted ≥ 98% of those in addition to syringol, sinapyl alcohol, coniferyl alcohol, coniferyl aldehyde, ferulic acid, vanillin, methyl vanillate, vanillyl alcohol and acetovanillone. Both enzymes showed high conversion yields towards guaiacyl-type phenols. Wild-type and 6E10 averaged 47% and 77% conversion yields for syringyl-type phenolics, 69% and 91% for guaiacyl-type phenolics, and 33% and 58% for hydroxybenzene-type phenolic compounds, respectively.

3.3. Catalytic parameters for the lignin-related phenolic substrates

Each substrate's maximal wavelength and molar extinction coefficient were determined (Supplementary Table S1) and used afterwards to measure enzymatic activities and estimate catalytic parameters (Table 3). It was not possible to set up colorimetric assays to measure the activity for 7 of the 24 phenolic substrates (vanillyl alcohol, acetovanillone, m-coumaric acid, 3,4-hydroxybenzoic, 4-hydroxybenzoic acid, gallic acid, and 4-hydroxyacetophenone). The catalytic parameters were estimated for 17 substrates using wild-type and 6E10 at the optimal pH of the enzymes. Wild-type oxidized all phenolics at the same order of magnitude; the average *k*_{cat} values for syringyl, guaiacyl and hydroxybenzene phenolics are comparable: 0.056 s⁻¹, 0.063 s⁻¹, and 0.08 s⁻¹, whereas the *K*_m values range from 0.01 to 1 mM (Table 3). In contrast, 6E10 showed a clear preference for syringyl-type compounds, which are oxidized at considerably higher rates, showing an average *k*_{cat} of 1.44 s⁻¹, as compared to 0.4 s⁻¹ for guaiacyl and 0.12 s⁻¹ for the hydroxybenzene phenolics. Thus, the activity improvements in the evolved variant are more prominent for the syringyl-type compounds (Table 3), which might be related to the fact that syringol was the substrate used during the activity screenings in the directed evolution of

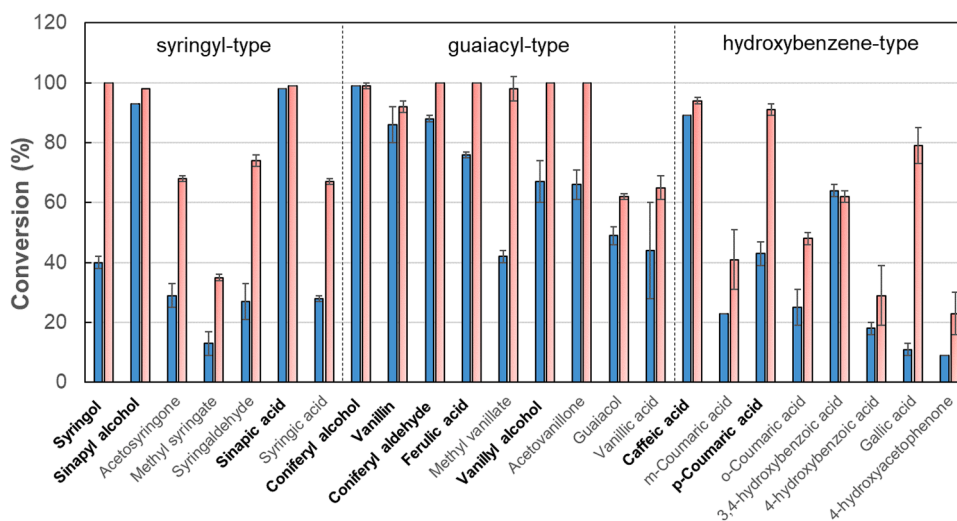


Fig. 1. Substrate conversion yields measured by HPLC after 24 h of reaction with wild-type (blue) and 6E10 variant (red), using 0.5 mM of phenolics at pH 4 and pH 8, respectively. Reactions started by addition of 0.5 mM H₂O₂. The substrates selected for product identification are in bold.

Table 3

Apparent steady-state kinetic parameters for the oxidation of phenolic substrates by PpDyP WT and 6E10, in the presence of 0.5 mM H₂O₂, at the optimal pH of each enzyme.

	Wild-type (pH 4)			6E10 (pH 8)		
	k_{cat} (s ⁻¹)	K_m (mM)	k_{cat}/K_m (M ⁻¹ s ⁻¹)	k_{cat} (s ⁻¹)	K_m (mM)	k_{cat}/K_m (M ⁻¹ s ⁻¹)
Syringyl-type phenolics						
Syringol	0.05 ± 0.01	0.70 ± 0.20	7.1 × 10 ²	3.5 ± 0.1	0.08 ± 0.06	4.3 × 10 ⁴
Sinapyl Alcohol	0.14 ± 0.01	0.04 ± 0.01	3.5 × 10 ³	2.2 ± 0.3	0.32 ± 0.09	6.8 × 10 ³
Methyl syringate	0.05 ± 0.01	0.08 ± 0.02	2.5 × 10 ²	1.7 ± 0.7	1.20 ± 0.70	1.4 × 10 ³
Acetosyringone	0.03 ± 0.01	0.05 ± 0.02	6.0 × 10 ²	0.9 ± 0.1	0.22 ± 0.05	4.1 × 10 ³
Syringaldehyde	0.01 ± 0.01	0.04 ± 0.01	2.5 × 10 ²	0.7 ± 0.03	0.010 ± 0.001	7.0 × 10 ⁴
Sinapic Acid	0.05 ± 0.01	0.03 ± 0.05	1.6 × 10 ³	0.4 ± 0.02	0.08 ± 0.01	5.0 × 10 ³
Syringic Acid	0.060 ± 0.01	0.15 ± 0.05	4.0 × 10 ²	0.7 ± 0.03	0.08 ± 0.01	8.8 × 10 ³
Guaiacyl-type phenolics						
Coniferyl alcohol	0.12 ± 0.03	0.3 ± 0.1	4.0 × 10 ²	0.3 ± 0.01	0.019 ± 0.004	1.6 × 10 ⁴
Vanillin	nd	–	–	0.7 ± 0.5	0.8 ± 0.5	8.8 × 10 ²
Coniferyl aldehyde	nd	–	–	0.10 ± 0.01	0.050 ± 0.009	2.0 × 10 ³
Ferulic acid	0.020 ± 0.002	0.015 ± 0.01	1.3 × 10 ⁴	0.10 ± 0.01	0.11 ± 0.03	0.9 × 10 ⁴
Methyl vanillate	nd	–	–	0.20 ± 0.04	0.33 ± 0.13	6.1 × 10 ²
Guaiacol	0.05 ± 0.01	0.01 ± 0.001	0.9 × 10 ³	0.50 ± 0.02	0.030 ± 0.003	1.9 × 10 ⁴
Vanillic acid	nd	–	–	1.0 ± 0.2	0.24 ± 0.1	4.7 × 10 ³
Hydroxybenzene-type phenolics						
Caffeic acid	0.080 ± 0.008	0.09 ± 0.03	8.9 × 10 ²	0.27 ± 0.05	0.3 ± 0.1	9.0 × 10 ²
p-coumaric acid	nd	–	–	0.06 ± 0.003	0.09 ± 0.02	6.6 × 10 ²
o-coumaric acid	nd	–	–	0.02 ± 0.001	0.15 ± 0.02	1.3 × 10 ²

nd: not detected

this enzyme, confirming the rule that “you get what you screen for”. In general, the increased activity of 6E10, as compared to the wild-type, was accompanied by a decrease in substrate affinity as assessed by the K_m values (Table 3). Nevertheless, 2–100-fold improved catalytic efficiencies (k_{cat}/K_m) of 6E10 were estimated for all substrates except ferulic and caffeic acids, which showed comparable efficiencies to the wild-type. In that context, 6E10 is the only unique DyP that offers maximal rates at pH 8–8.5. It is also a better biocatalyst for lignin-related phenolics (3.5 s⁻¹ for syringol versus wild-type 0.05 s⁻¹) than other bacterial DyPs reported in the literature. For example, activities of around 0.03–0.5 U/mg were measured for syringol in DyPs from *Saccharomonospora viridis* [36], *Streptomyces avermitilis* [37], *Enterobacter lignolyticus* (for guaiacol an activity of 0.34 U/mg [38]), *Thermobifida fusca* [39] and *Bacillus subtilis* [29]. Fungal DyPs, such as those found in *Irpex lacteus*, *A. auricula-judae* or *P. ostreatus*, exhibit k_{cat} values 10–100 orders of magnitude higher than 6E10; however, these are highly acidic enzymes, operating at an optimum pH between 2 and 3.5, which is a setback for their industrial application [40].

There is no clear trend between chemical and enzymatic oxidation of the lignin-related phenolics tested other than the preference for pH 8.0 and syringyl-type substrates (Tables 2 and 3). Sinapic acid, with the lowest value of E_{pa} at pH 8.0 (0.63 V), displays the lowest turnover rate of the syringyl type family (0.4 s⁻¹). Substrates such as syringol, coniferyl alcohol and coniferyl aldehyde, although sharing similar redox potentials (0.68–0.69 V), are oxidized at different rates: 6E10 oxidized syringol 20 and 60-fold faster than coniferyl alcohol and coniferyl aldehyde. The coumaric acid series (*p*-, *o*-, and *m*-coumaric acid) indicates well the effect of the position of the substituents on the phenolic ring on the enzymatic oxidation rates, following the order *p*-coumaric acid > *o*-coumaric acid > *m*-coumaric acid, with 6E10 oxidizing the *p*-substituent at 3-fold higher rates than the *o*-substituent and showing no measurable activity for the *m*-substituent. The observed differences are therefore expected to result from specific substrate-enzyme interactions, e.g. accommodation of substrates to the binding site(s), distance to the heme, electron transfer rates and product dissociation.

3.4. Identification of products of reactions

A set of 11 substrates was selected from those that were oxidized at higher rates and showed > 90% conversion yields (syringol, sinapyl alcohol, sinapic acid, coniferyl alcohol, vanillin, vanillyl alcohol, acetovanillone, ferulic acid, caffeic acid and *p*-coumaric acid) for reactions to identify and characterize the products of reactions. Reactions monitored after 1 h by HPLC revealed no differences when compared to the 24 h reactions in substrate conversion yields (Supplementary Fig. S3). The ESI-MS results confirmed that the transformation was incomplete for some substrates (vanillin, vanillyl alcohol, acetovanillone, ferulic acid, and coumaric acid). In general, the product signals obtained were consistent with the formation of dimeric structures with molecular weights of ($2 \times MW_{\text{substrate}} - 2H$), except for coniferyl aldehyde, for which no relevant signals were found (Table 4). Similar to laccases, DyPs mediate the one-electron oxidation of phenolics resulting in formation of radical intermediates or quinones that are subsequently coupled with other substrate molecules. The direction taken by the radical coupling reactions depends on the substitution pattern of the aromatic ring, reflecting the influence of electronic features on the stabilization and chemical reactivity of the first formed radical. Various stereo- and regioisomers can be considered, as the same m/z values were found at different retention times, indicating the presence of different dimeric isomers. The oxidation of the non-phenolic hydroxy group to the aldehyde was also observed in the reaction of 6E10 with sinapyl alcohol, coniferyl alcohol, and vanillyl alcohol.

The oxidation of syringol showed a peak at m/z 307, which is consistent with the molecular formula $C_{16}H_{18}O_6$ and can be attributed to C-C, C-O, or O-O dimers (Supplementary Fig. S4), although the fragmentation pattern is inconsistent with C-C and C-O dimers [23,41,42]. Enzymatic reactions of syringaldehyde, methylsyringate and acetosyringone with bacterial CotA-laccase suggest that the main radical coupling route for the oxidation of the phenolics involves the formation of dimeric and trimeric structures arising from the C-O coupling reactions, with a release, in some cases, of an aromatic substituent group [43]. The MS data for reaction products with guaiacyl-type derivatives, vanillyl alcohol, vanillin and acetovanillone showed the formation of at least one dimeric structure. Furthermore, the oxidation of the non-phenolic hydroxyl group of vanillyl alcohol was observed with the formation of vanillin. In the reaction with vanillin, the peak at m/z 303 is consistent with the molecular formula $C_{16}H_{14}O_6$ and was attributed to divanillin (5,5' dimer) or the 4-O-5 isomer. The 1H NMR analysis of the scale-up reaction with vanillin confirmed the incomplete oxidation of the substrate and the identification of both 5,5' and 4-O-5 dimers at low yields (~10%) (see Supplementary Table S3). Considering these results, for acetovanillone, the peak at m/z 331 is consistent with the molecular formula $C_{18}H_{18}O_6$ and can be assigned to diapocynin or its C-O isomer. Divanillin is a taste enhancer [44] and flavoring, and diapocynin, the dimer of acetovanillone, has important anti-inflammatory and neuroprotective effects [45]. Furthermore, both compounds are valuable intermediates for synthesis of polymers, such as polyvanillin, Schiff bases and conjugated polymers [7,25,27]. The production of both divanillin and diapocynin using laccases and horseradish peroxidase was previously reported [44,46]. The production of divanillin was also observed using one pot, two-step cascade reactions catalyzed by a fusion of eugenol oxidase with the SviDyP from *Saccharomonospora viridis* DSM 43017 [47]. The fusion enzyme was able to oxidize vanillyl alcohol to vanillin due to the oxidase, while the DyP dimerized vanillin to divanillin.

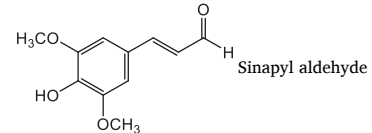
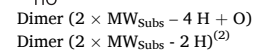
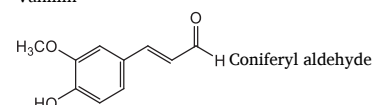
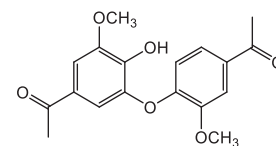
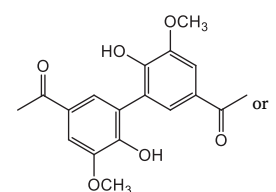
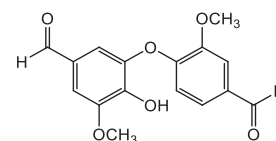
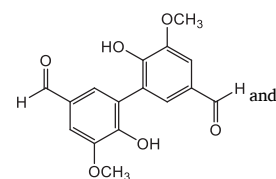
In the case of phenylpropanoid type monomers (for example, coniferyl alcohol, sinapic acid, caffeic acid and *p*-coumaric acid), the m/z values found are compatible with a higher number of dimeric structures (Table 4 and Supplementary Figs S5-S9). The oxidation of these lignan and neolignan precursors to the corresponding phenoxy radicals can undergo delocalization along the unsaturated backbone leading to different resonance forms involving carbon atoms (Scheme 2A).

Different pathways involving free-radical coupling at the O-4, 5- and 8-positions after that lead to the formation of lignan and neolignan dimers and oligomers, where linkages between subunits involve either C-C (5,5'-, 8,5'- and 8,8'-dimers) or C-O (8-O-4 and 4-O-5-dimers) bonds (Scheme 2B). Moreover, the ratio of the different coupled dimers is strongly dependent on the pH and other experimental conditions, such

Table 4

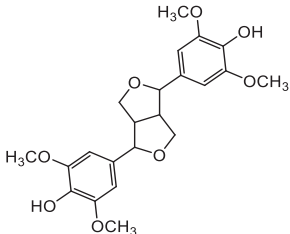
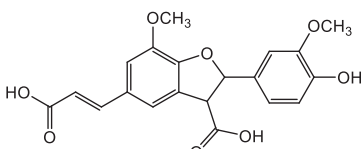
ESI-MS (positive mode) data and retention times (rt) for 6E10 reactions with substrates at pH 8 and putative products.

Substrate	rt (min)	m/z (+)	Attribution
Guaiacyl and Syringyl type derivatives			
Syringol	8.32	307	Dimer ($2 \times MW_{\text{Subs}} - 2H$) ⁽¹⁾
Vanillyl alcohol	5.83	137	Vanillyl alcohol
Vanillyl alcohol	6.64	289	Dimer ($2 \times MW_{\text{Subs}} - 2H$) - 18
	7.08	153	Vanillin
	9.42	549	-
	8.52	303	Dimer ($2 \times MW_{\text{Subs}} - 2H$)
Vanillin	7.05	153	Vanillin
Vanillin	7.99	468	-
	8.52	303	Dimer ($2 \times MW_{\text{Subs}} - 2H$)
	8.52	303	Dimer ($2 \times MW_{\text{Subs}} - 2H$)
Acetovanillone			
Acetovanillone	8.65	469	-
	7.31	167	Acetovanillone
	8.65	331	Dimer ($2 \times MW_{\text{Subs}} - 2H$)
Lignan and neolignan type derivatives			
Coniferyl alcohol	7.07	153	Vanillin
Coniferyl alcohol	7.83	179	-
	8.86	511	-
Sinapyl alcohol	8.09	373	Dimer ($2 \times MW_{\text{Subs}} - 4H + O$)
	8.11	359	Dimer ($2 \times MW_{\text{Subs}} - 2H$) ⁽²⁾
	6.65	209	-
Sinapyl alcohol	7.32	405	-
	8.36	419	-



(continued on next page)

Table 4 (continued)

Substrate	rt (min)	<i>m/z</i> (+)	Attribution
			Dimer (2 × MW _{Subs} - 2 H)
			
p-Coumaric acid	9.61	417	Dehydrodimer (2 × MW _{Subs} - 4 H)
	7.03	165	p-coumaric acid
	7.61	327	Dimer (2 × MW _{Subs} - 2 H) ⁽³⁾
	8.37	327	Dimer (2 × MW _{Subs} - 2 H) ⁽³⁾
Caffeic acid	8.53	327	Dimer (2 × MW _{Subs} - 2 H) ⁽³⁾
	7.40	359	Dimer (2 × MW _{Subs} - 2 H) ⁽⁴⁾
	7.60	359	Dimer (2 × MW _{Subs} - 2 H) ⁽⁴⁾
	7.71	359	Dimer (2 × MW _{Subs} - 2 H) ⁽⁴⁾
Ferulic acid	7.93	359	Dimer (2 × MW _{Subs} - 2 H) ⁽⁴⁾
	7.25	179	Ferulic acid
	7.39	369	–
	8.37	387	Dimer (2 × MW _{Subs} - 2 H) ⁽⁵⁾
			
Sinapic acid	9.37	373	–
	7.20	447	Dimer (2 × MW _{Subs} - 2 H) ⁽⁶⁾
	8.07	447	Dimer (2 × MW _{Subs} - 2 H) ⁽⁶⁾

(¹) see Fig. S4; (²) see Fig S5; (³) see Fig S6; (⁴) see Fig S7; (⁵) see Fig. S8; (⁶) see Fig. S9

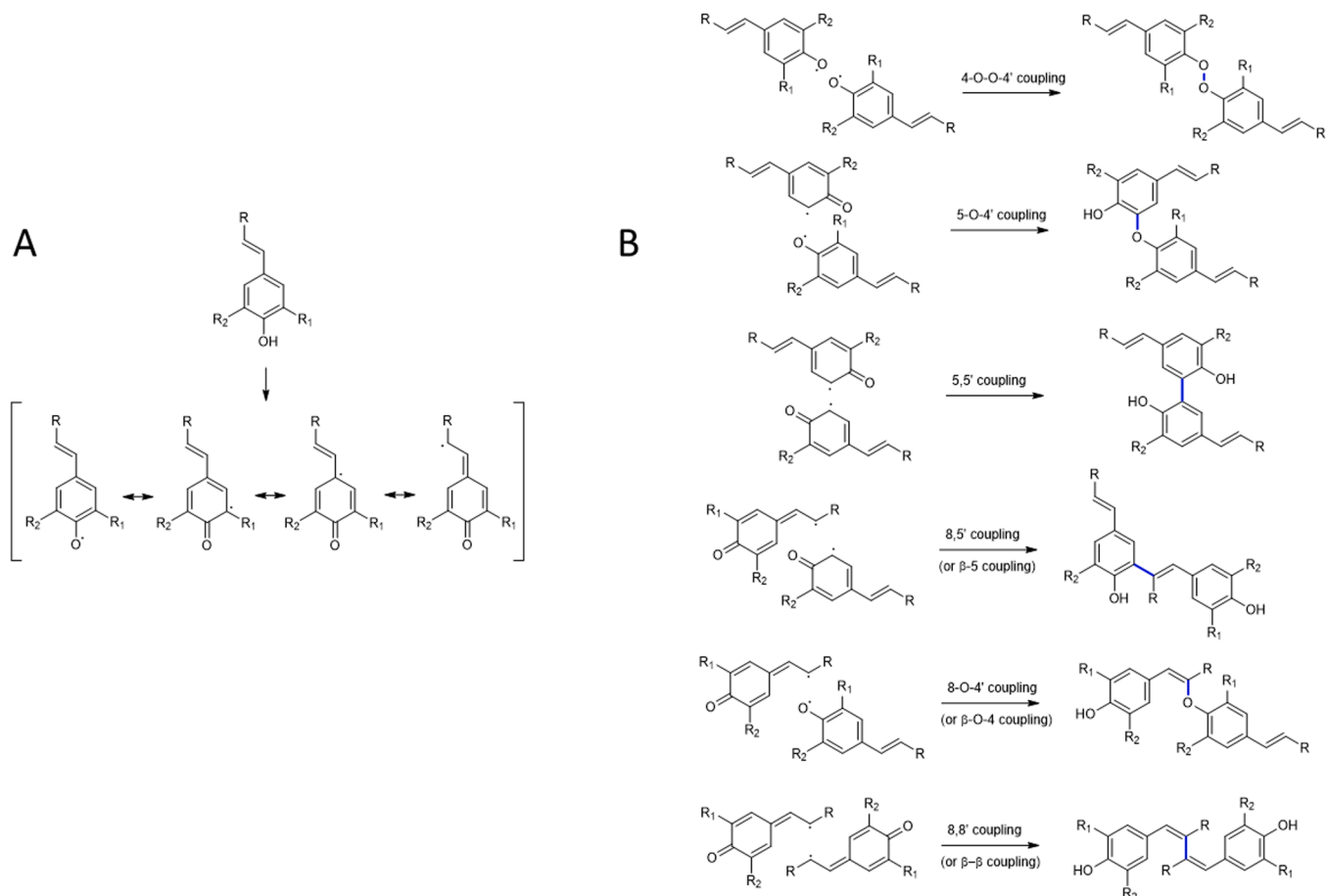
as the substrate supply rate, the presence of co-solvents and reaction time [48–50].

After enzymatic oxidation of coniferyl alcohol, four peaks can be distinguished after one-hour of reaction and attributed to vanillin (rt = 7.07 min, *m/z* 153), coniferyl aldehyde (rt = 7.83 min, *m/z* 179) resulting from the oxidation of the non-phenolic group, and a dimeric product eluting at 8.09 min for which different radical coupling isomers have been considered (see Supplementary Fig. S5). A similar behavior was found for sinapyl alcohol oxidation where several peaks with varying retention times were detected at 6.65 min (*m/z* 209; C₁₁H₁₂O₄) attributed to sinapyl aldehyde, 7.32 min (*m/z* 405; C₂₁H₂₄O₈); 8.36 min (*m/z* 419; C₂₂H₂₆O₈) and 9.61 min (*m/z* 417; C₂₂H₂₄O₈). Considering the principal radical coupling reactions within the syringyl type monomers, the 8,8' and 8-O-4 couplings, the peaks at *m/z* 419 and *m/z* 417 can be assigned to lignan dimeric structures (2 × MW-2 H) and (2 × MW-4 H) respectively. The ¹H NMR analysis of a reaction with sinapyl alcohol using 6E10 indicated the complete oxidation of the substrate and the formation of the lignan syringaresinol as the main product, confirming the structure of the 8,8' (or β-β dimer (2 × MW - 2 H) proposed from the MS analysis (Supplementary Table S3). The neolignan 8-O-4 dimer was not detected by either MS or NMR analysis. The enzymatic synthesis of syringaresinol, a furofuran lignan dimer formed upon oxidation of sinapyl alcohol, was previously described using the *Trametes versicolor* laccase [50] and one-pot conversion using eugenol oxidase and horseradish peroxidase [50]. Syringaresinol displays interesting bioactivity properties [50–52] and is also of interest in replacing bisphenol A for polymer synthesis [25,53–55]. Although available naturally in plants, syringaresinol is isolated from natural

sources in only meager yields [56]. The enzymatic reactions with hydroxyphenyl and guaiacyl type derivatives *p*-coumaric, caffeic and ferulic acids are characterized by the production of multiple dimeric isomers, eluted at different retention times, and showing different mass fragmentation patterns, and reflect the coupling possibilities of the primary formed radicals (Scheme 2), their relative stability, and their dependence on critical parameters and reaction conditions [48,57]. The product profile of the *p*-coumaric acid reaction is complex. The presence of three different dimer isomers *m/z* 327 (consistent with the molecular formula C₁₈H₁₄O₆) at different retention times indicates the formation of different isomers (see Supplementary Fig. S6). Mass fragmentation data showed, in all cases, losses of one or two neutral water, CO and CO₂ molecules. However, the differences in MS fragmentation patterns did not allow for distinguishing a particular isomer. The same result was obtained for caffeic acid, where four products can be determined, all isomers of *m/z* 359 (see Supplementary Fig. S7 for the dimeric structures considered). For sinapic acid, two isomers of the dimer *m/z* 447 eluted at rt 7.20 and 8.07 min. Although several structural isomers can be regarded as possible (see supplementary Fig. S9), the MS fragmentation patterns in both cases did not allow the attribution of a particular isomer. A different result was obtained for ferulic acid since the reaction was incomplete after one hour, and only one dimer at rt 8.37 min (*m/z* 387 consistent with the molecular formula C₂₀H₁₈O₈) was present. Although a high number of dimeric structures can be considered (see supplementary Fig. S8), the comparison between the mass fragmentation pattern of this dimer and the literature data for diferulates strongly points to the neolignan 8,5' benzofurandehydroferulic acid dimer as the oxidation product [58]. This dimer is a potential biomarker in several food products, such as wheat, corn and rye, and shows antioxidant properties [59].

4. Concluding remarks

All lignin-derived phenolics tested were oxidized by PpDyP wild-type and the 6E10 variant at pH 4 and pH 8, respectively. Kinetic measurements show that the turnover rate of 6E10 was higher across the board, resulting in higher catalytic efficiency for all substrates tested. When substrate conversion after 24 h was analyzed, differences were less pronounced, and both enzymes could oxidize the tested substrates to comparable extents. While the actual physiological functions of DyPs have yet to be elucidated, the wealth of their catalyzed reactions is undoubtedly interesting from environmental and industrial points of view. Radicals resulting from phenolic oxidation are involved in homo-coupling or cross-coupling reactions resulting in homo- or heterodimers, oligomers and even polymers at long incubation times [60]. Reactions of 6E10 with phenolic substrates tend to form dimers by radical coupling, as assessed after identifying reaction products by MS; dimers such as divanillin, diapocynin and the lignan syringaresinol, are interesting biologically active molecules with potential applications such as building blocks for the resins industry or food additives (divanillin), as pharmaceuticals (diapocynin) or as a starting material in the polymer industry (syringaresinol). These are natural products in plant extracts that show interesting biological activity (e.g. anti-inflammatory and anti-cancer properties) but whose extraction suffers from low yields. Structurally diverse products can be obtained through electron delocalizing phenolic radicals before coupling. Future studies need to focus on testing reaction conditions that lead to the control of the reaction into the desired path, i.e. that allow the control of the distribution of the products and the concomitant improvement of the reaction yields. Unveiling the molecular basis of chemical stereo- and region-specificity of monolignol-derived radical-radical coupling leading to lignans, neolignans and other dimeric structures will represent a robust knowledge and significant advance beyond the state-of-the-art in combinatorial lignin chemistry, with critical reflection in eco-friendly lignin valorization that supports the economic sustainability of lignocellulose biorefineries.



Scheme 2. (A) Proposed radical species originated from substituted phenylpropanoid derivatives oxidation (R₁, R₂ = H, OCH₃). (B) Overview of possible lignan and neolignan type dimers formed after DyP-type peroxidase oxidation of phenylpropanoid derivatives.

Funding

This work was supported by the Fundação para a Ciência e Tecnologia, Portugal, grants PTDC/BBE/BB/0122/2014, PTDC/BII-BBF/29564/2017, MOSTMICRO-ITQB (UIDB/04612/2020 and UIDP/04612/2020), LS4FUTURE Associated Laboratory (LA/P/0087/2020), projects UIDB/00100/2020, UIDP/00100/2020, Institute of Molecular Sciences (IMS) Associate Laboratory (project LA/P/0056/2020). DS acknowledges FCT Ph.D. Fellowship SFRH/BD/132702/2017.

Declarations of interest

None.

Acknowledgments

The authors thank João Zagalo Pereira, Sónia Mendes, and Vânia Brissos for their help in preliminary investigations.

Appendix A. Supporting information

Supplementary data associated with this article can be found in the online version at [doi:10.1016/j.nbt.2022.12.003](https://doi.org/10.1016/j.nbt.2022.12.003).

References

- [1] Sugano Y. DyP-type peroxidases comprise a novel heme peroxidase family. *Cell Mol Life Sci* 2009;66:1387–403.
- [2] Colpa DJ, Fraaije MW, van Bloois E. DyP-type peroxidases: a promising and versatile class of enzymes. *J Ind Microbiol Biotechnol* 2014;41:1–7.
- [3] Floudas D, Binder M, Riley R, Barry K, Blanchette RA, Henrissat B, et al. The Paleozoic origin of enzymatic lignin decomposition reconstructed from 31 fungal genomes. *Science* 2012;336:1715–9.
- [4] Ruiz-Duenas FJ, Lundell T, Floudas D, Nagy LG, Barrasa JM, Hibbett DS, et al. Lignin-degrading peroxidases in Polyporales: an evolutionary survey based on 10 sequenced genomes. *Mycologia* 2013;105:1428–44.
- [5] Linde D, Ruiz-Duenas FJ, Fernandez-Fueyo E, Guallar V, Hammel KE, Pogni R, et al. Basidiomycete DyPs: genomic diversity, structural-functional aspects, reaction mechanism and environmental significance. *Arch Biochem Biophys* 2015; 574:66–74.
- [6] Kellner H, Luis P, Pecyna MJ, Barbi F, Kapturska D, Kruger D, et al. Widespread occurrence of expressed fungal secretory peroxidases in forest soils. *PLoS One* 2014;9:e95557.
- [7] Sun Z, Fridrich B, de Santi A, Elangovan S, Barta K. Bright side of lignin depolymerization: toward new platform chemicals. *Chem Rev* 2018;118:614–78.
- [8] Cao Y, Chen SS, Zhang S, Ok YS, Matsagar BM, Wu KC, et al. Advances in lignin valorization towards bio-based chemicals and fuels: lignin biorefinery. *Bioresour Technol* 2019;291:121878.
- [9] Van den Bosch S, Koelewijn SF, Renders T, Van den Bossche G, Vangeel T, Schutyser W, et al. Catalytic strategies towards lignin-derived chemicals. *Top Curr Chem* 2018;376:36.
- [10] Abu-Omar MM, Barta K, Beckham GT, Luterbacher JS, Ralph J, Rinaldi R, et al. Guidelines for performing lignin-first biorefining. *Energy Environ Sci* 2021;14: 262–92.
- [11] Stone ML, Anderson EM, Meek KM, Reed M, Katahira R, Chen F, et al. Reductive catalytic fractionation of C-lignin. *ACS Sustain Chem Eng* 2018;6:11211–8.
- [12] Cao LC, Yu IKM, Liu YY, Ruan XX, Tsang DCW, Hunt AJ, et al. Lignin valorization for the production of renewable chemicals: state-of-the-art review and future prospects. *Bioresour Technol* 2018;269:465–75.
- [13] Ragauskas AJ, Beckham GT, Biddy MJ, Chandra R, Chen F, Davis MF, et al. Lignin valorization: improving lignin processing in the biorefinery. *Science* 2014;344: 1246843.
- [14] Gall DL, Ralph J, Donohue TJ, Noguera DR. Biochemical transformation of lignin for deriving valued commodities from lignocellulose. *Curr Opin Biotechnol* 2017; 45:120–6.
- [15] Linger JG, Vardon DR, Guarnieri MT, Karp EM, Hunsinger GB, Franden MA, et al. Lignin valorization through integrated biological funneling and chemical catalysis. *Proc Natl Acad Sci USA* 2014;111:12013–8.

- [16] Borchert AJ, Henson WR, Beckham GT. Challenges and opportunities in biological funneling of heterogeneous and toxic substrates beyond lignin. *Curr Opin Biotechnol* 2022;73:1–13.
- [17] Schutyser W, Renders T, Van den Bosch S, Koelewijn SF, Beckham GT, Sels BF. Chemicals from lignin: an interplay of lignocellulose fractionation, depolymerisation, and upgrading. *Chem Soc Rev* 2018;47:852–908.
- [18] Runeberg PA, Brusentsev Y, Rendon SMK, Eklund PC. Oxidative transformations of lignans. *Molecules* 2019;24:300.
- [19] Hamalainen V, Gronroos T, Suonpaa A, Hekkila MW, Romein B, Ihalainen P, et al. Enzymatic processes to unlock the lignin value. *Front Bioeng Biotechnol* 2018;6:20.
- [20] Hammel KE, Cullen D. Role of fungal peroxidases in biological ligninolysis. *Curr Opin Plant Biol* 2008;11:349–55.
- [21] Kudanga T, Nemadziva B, Le Roes-Hill M. Laccase catalysis for the synthesis of bioactive compounds. *Appl Microbiol Biotechnol* 2017;101:13–33.
- [22] Natte K, Narani A, Goyal V, Sarki N, Jagadeesh RV. Synthesis of functional chemicals from lignin-derived monomers by selective organic transformations. *Adv Synth Catal* 2020;362:5143–69.
- [23] Adelakun OE, Kudanga T, Green IR, Le Roes-Hill M, Burton SG. Enzymatic modification of 2,6-dimethoxyphenol for the synthesis of dimers with high antioxidant capacity. *Process Biochem* 2012;47:1926–32.
- [24] Zalesak F, Bon DJD, Pospisil J. Lignans and Neolignans: plant secondary metabolites as a reservoir of biologically active substances. *Pharmacol Res* 2019;146:104284.
- [25] Llevot A, Grau E, Carlotti S, Grelier S, Cramail H. From lignin-derived aromatic compounds to novel biobased polymers. *Macromol Rapid Commun* 2016;37:9–28.
- [26] Bass GF, Epps TH. Recent developments towards performance-enhancing lignin-based polymers. *Polym Chem* 2021;12:4130–58.
- [27] Fang Z, Nikafshar S, Hegg EL, Nejad M. Biobased divanillin as a precursor for formulating biobased epoxy resin. *ACS Sustain Chem Eng* 2020;8:9095–103.
- [28] Upton BM, Kasko AM. Strategies for the conversion of lignin to high-value polymeric materials: review and perspective. *Chem Rev* 2016;116:2275–306.
- [29] Santos A, Mendes S, Brissos V, Martins LO. New dye-decolorizing peroxidases from *Bacillus subtilis* and *Pseudomonas putida* MET94: towards biotechnological applications. *Appl Microbiol Biotechnol* 2014;98:2053–65.
- [30] Brissos V, Tavares D, Sousa AC, Robalo MP, Martins LO. Engineering a bacterial DyP-type peroxidase for enhanced oxidation of lignin-related phenolics at alkaline pH. *ACS Catal* 2017;7:3454–65.
- [31] Rosado T, Bernardo P, Koci K, Coelho AV, Robalo MP, Martins LO. Methyl syringate: an efficient phenolic mediator for bacterial and fungal laccases. *Bioresour Technol* 2012;124:371–8.
- [32] Ragnar M, Lindgren CT, Nilvebrant NO. pK(a)-values of guaiacyl and syringyl phenols related to lignin. *J Wood Chem Technol* 2000;20:277–305.
- [33] Erdemgil FZ, Sanli S, Sanli N, Ozkan G, Barbosa J, Guiteras J, et al. Determination of pK(a) values of some hydroxylated benzoic acids in methanol-water binary mixtures by LC methodology and potentiometry. *Talanta* 2007;72:489–96.
- [34] Genaro-Mattos TC, Mauricio AQ, Rettori D, Alonso A, Hermes-Lima M. Antioxidant activity of caffeic acid against iron-induced free radical generation—a chemical approach. *PLoS One* 2015;10:e0142402.
- [35] Benvindi A, Dadras A, Abbasi S, Tezerjani MD, Rezaeinasab M, Tabaraki R, et al. Experimental and computational study of the pK(a) of coumaric acid derivatives. *J Chin Chem Soc* 2019;66:589–93.
- [36] Yu W, Liu W, Huang H, Zheng F, Wang X, Wu Y, et al. Application of a novel alkali-tolerant thermostable DyP-type peroxidase from *Saccharomonospora viridis* DSM 43017 in biobleaching of eucalyptus kraft pulp. *PLoS One* 2014;9:e110319.
- [37] Sugawara K, Nishihashi Y, Narioka T, Yoshida T, Morita M, Sugano Y. Characterization of a novel DyP-type peroxidase from *Streptomyces avermitilis*. *J Biosci Bioeng* 2017;123:425–30.
- [38] Shrestha R, Huang GC, Meekins DA, Geisbrecht BV, Li P. Mechanistic insights into dye-decolorizing peroxidase revealed by solvent isotope and viscosity effects. *ACS Catal* 2017;7:6352–64.
- [39] Rahmanpour R, Rea D, Jamshidi S, Fulop V, Bugg TD. Structure of *Thermobifida fusca* DyP-type peroxidase and activity towards Kraft lignin and lignin model compounds. *Arch Biochem Biophys* 2016;594:54–60.
- [40] Eugenio LI, Peces-Pérez R, Linde D, Prieto A, Barriuso J, Ruiz-Dueñas FJ, Martínez MJ. Characterization of a Dye-decolorizing peroxidase from *Irpex lacteus* expressed in *Escherichia coli*: an enzyme with wide substrate specificity able to transform lignosulfonates. *J Fungus* 2015;99:8927–42.
- [41] Schirmann JG, Dekker RFH, Borsato D, Barbosa-Dekker AM. Selective control for the laccase-catalyzed synthesis of dimers from 2,6-dimethoxyphenol: optimization of 3,3',5,5'-tetramethoxy-biphenyl-4,4'-diol synthesis using factorial design, and evaluation of its antioxidant action in biodiesel. *Appl Catal A Gen* 2018;555:88–97.
- [42] Sun Z, Yang YQ, Xu XL, Sheng CY, Hou ZX, Ding F. [Analysis of aerosol concentration characteristics under continuous synoptic systems in Qingdao]. *Huan Jing Ke Xue* 2010;31:871–6.
- [43] Rosado T, Bernardo P, Koci K, Coelho AV, Robalo MP, Martins LO. Methyl syringate: an efficient phenolic mediator for bacterial and fungal laccases. *Bioresour Technol* 2012;124:371–8.
- [44] Krings U, Espan V, Berger RG. The taste enhancer divanillin: a review on sources and enzymatic generation. *Flavour Frag J* 2015;30:362–5.
- [45] Ismail HM, Scapozza L, Ruegg UT, Dorchies OM. Diapocynin, a dimer of the NADPH oxidase inhibitor apocynin, reduces ros production and prevents force loss in eccentrically contracting dystrophic muscle. *PLoS One* 2014;9:e110708.
- [46] Nishimura RT, Giammanco CH, Vosburg DA. Green, enzymatic syntheses of divanillin and diapocynin for the organic, biochemistry, or advanced general chemistry laboratory. *J Chem Educ* 2010;87:526–7.
- [47] Colpa DI, Loncar N, Schmidt M, Faaïje MW. Creating oxidase–peroxidase fusion enzymes as a toolbox for cascade reactions. *ChemBioChem* 2017;18:2226–30.
- [48] Gruz J, Pospisil J, Kozubikova H, Pospisil T, Dolezal K, Bunzel M, et al. Determination of free diferulic, disinapic and dicoumaric acids in plants and foods. *Food Chem* 2015;171:280–6.
- [49] Jaufurally AS, Teixeira A, Ducrot PH, Allais F. Chemo-enzymatic synthesis and functionalization of syringaresinol: a promising biobased antiradical additive and platform for bisphenolic monomers. *Abstr Pap Am Chem Sci* 2016:252.
- [50] Jaufurally AS, Teixeira ARS, Hollande L, Allais F, Ducrot PH. Optimization of the laccase-catalyzed synthesis of (+/-)-syringaresinol and study of its thermal and antiradical activities. *Chemistryselect* 2016;1:5165–71.
- [51] Habib M, Trajkovic M, Faaïje MW. The biocatalytic synthesis of syringaresinol from 2,6-dimethoxy-4-allylphenol in one-pot using a tailored oxidase/peroxidase system. *ACS Catal* 2018;8:5549–52.
- [52] Bajpai VK, Alam MB, Quan KT, Ju MK, Majumder R, Shukla S, et al. Attenuation of inflammatory responses by (+)-syringaresinol via MAP-Kinase-mediated suppression of NF-kappa B signaling in vitro and in vivo. *Sci Rep* 2018;8:9216.
- [53] Janvier M, Hollande L, Jaufurally AS, Pernes M, Menard R, Grimaldi M, et al. Syringaresinol: a renewable and safer alternative to bisphenol A for epoxy-amine resins. *Chem Sus Chem* 2017;10:738–46.
- [54] Janvier M, Hollande L, Jaufurally AS, Ducrot PH, Allais F. Syringaresinol: a new bio-based bisphenolic building-block for polymers synthesis. *Abstr Pap Am Chem Sci* 2016:252.
- [55] Chio CL, Sain M, Qin WS. Lignin utilization: a review of lignin depolymerization from various aspects. *Renew Sustain Energy Rev* 2019;107:232–49.
- [56] Monthong W, Pitchuanom S, Nuntasana N, Pompimon W. (+)-Syringaresinol lignan from new species magnolia thailandica. *Am J Appl Sci* 2011;8:1268–71.
- [57] Flourat AL, Zeaiter N, Vallee E, Nguyen VPT, Fadlallah S, Allais F. A sustainable preparative-scale chemo-enzymatic synthesis of 6-hydroxy-5,7-dimethoxy-2-naphthoic acid (DMNA) from sinapic acid. *Green Chem Lett Rev* 2022;15:557–71.
- [58] Vismeh R, Lu F, Chundawat SP, Humpala JF, Azarpira A, Balan V, Dale BE, et al. Profiling of diferulates (plant cell wall cross-linkers) using ultrahigh-performance liquid chromatography-tandem mass spectrometry. *Analyst* 2013;138:6683–92.
- [59] Garcia-Conesa MT, Plumb GW, Kroon PA, Wallace G, Williamson G. Antioxidant properties of ferulic acid dimers. *Redox Rep* 1997;3:239–44.
- [60] Martins LO, Melo EP, Sanchez-Amat A, Robalo MP. Bacterial laccases: some recent advances and applications. In: Valorisation, Schlosser D, editors. *Laccases in bioremediation and waste*. Springer; 2020. p. 27–55.